

---

# Understanding and Exploiting Plasticity for Non-stationary Network Resource Adaptation

---

**Zhiqiang He**

The University of Electro-Communications  
hezhiqiang@ieee.org  
Tokyo, Japan

**Zhi Liu**

The University of Electro-Communications  
liu@ieee.org  
Tokyo, Japan

## Abstract

Adapting to non-stationary network conditions presents significant challenges for resource adaptation. However, current solutions primarily rely on stationary assumptions. While data-driven reinforcement learning approaches offer promising solutions for handling network dynamics, our systematic investigation reveals a critical limitation: neural networks suffer from plasticity loss, significantly impeding their ability to adapt to evolving network conditions. Through theoretical analysis of neural propagation mechanisms, we demonstrate that existing dormant neuron metrics inadequately characterize neural plasticity loss. To address this limitation, we have developed the Silent Neuron theory, which provides a more comprehensive framework for understanding plasticity degradation. Based on these theoretical insights, we propose the Reset Silent Neuron (ReSiN), which preserves neural plasticity through strategic neuron resets guided by both forward and backward propagation states. In our implementation of an adaptive video streaming system, ReSiN has shown significant improvements over existing solutions, achieving up to 168% higher bitrate and 108% better quality of experience (QoE) while maintaining comparable smoothness. Furthermore, ReSiN consistently outperforms in stationary environments, demonstrating its robust adaptability across different network conditions.

## 1 Introduction

In the field of Network Resource Adaptation, which encompasses applications such as adaptive multimedia streaming, computation offloading, and IoT communication, problems are typically modeled as constrained optimization problems under dynamic network environments [Hu et al. \(2024\)](#); [Huang et al. \(2021\)](#); [Li et al. \(2024b\)](#); [Mao et al. \(2017\)](#); [Meng et al. \(2021\)](#); [Zhao et al. \(2024\)](#). The objective is to maximize system performance (e.g., Quality of Service (QoS), quality of experience (QoE)) while satisfying constraints on bandwidth, latency, and energy consumption. Traditional research typically assumes a stationary network environment, where network bandwidth follows fixed probability distributions or fluctuates within certain bounds [Li et al. \(2024b\)](#); [Wang et al. \(2024b\)](#). While this assumption simplifies the problem and enables conventional optimization methods. However, real-world network environments, particularly in mobile scenarios and complex network topologies, inherently exhibit non-stationary characteristics [Cao et al. \(2001\)](#). Network bandwidth distributions can undergo dramatic changes, such as during transitions between 4G and WiFi networks or in congested regions. In practice, physical-layer mechanisms such as adaptive modulation and retransmission can help to reduce short-term fluctuations. However, they are not able to completely eliminate the non-stationarity that is often observed at the application layer. This is particularly true in situations where there is varying mobility, congestion, or network switching [Deng et al. \(2014\)](#); [Sun et al. \(2016\)](#); [Wu et al. \(2017\)](#). These non-stationary dynamics fundamentally transform the optimization problem, as both constraints and variables experience sudden changes, posing significant challenges to existing solutions [Liu et al. \(2021\)](#); [Patel et al. \(2024\)](#).

To gain a comprehensive understanding of the challenges presented by non-stationary environments, we analyze how three major categories of optimization approaches fail to handle sudden changes in network bandwidth conditions. Conventional optimization methods, such as Lyapunov optimization [Jia et al. \(2022\)](#) and model predictive control [Yin et al. \(2015\)](#), are unable to effectively handle these changes due to the invalidation of underlying system model assumptions. This results in frequent restarts of the optimization process. Similarly, heuristic algorithms are also ill-equipped to handle non-stationary environments as they rely on historical population information which becomes obsolete in the face of sudden changes, requiring reinitialization and numerous iterations to adapt. While reinforcement learning (RL) has emerged as a popular solution for network resource allocation problems, even state-of-the-art approaches face significant challenges in non-stationary environments [Hu et al. \(2024\)](#); [Huang et al. \(2021\)](#); [Patel et al. \(2024\)](#); [Wang et al. \(2024b\)](#). In classical reinforcement learning approaches for solving MDPs (Markov Decision Processes), variations in network bandwidth are typically modeled as a stationary distribution. Data-driven methods are then used to learn this distribution.

However, in non-stationary network environments, bandwidth changes are abrupt and do not follow a fixed distribution. This violates the assumptions of the standard MDP framework and requires the agent to quickly learn and adapt to multiple, shifting MDPs [Padakandla \(2021\)](#). Traditional RL methods struggle in non-stationary environments because the violation of the Markov property invalidates previously learned value functions and policies. As the environment shifts, both the stored experience in replay buffers and the network weights become outdated, leading to misaligned gradient updates and unstable learning dynamics. While this degradation has been empirically observed, the underlying mechanisms remain an active area of research [Lewandowski et al. \(2024\)](#). These effects result in a loss of plasticity and can ultimately cause complete learning collapse [Mao et al. \(2017\)](#); [Patel et al. \(2024\)](#).

Although not specifically targeting non-stationary environments, existing works have attempted to address network dynamics through either priority sampling [Patel et al. \(2024\)](#) or meta-learning approaches [Kan et al. \(2022\)](#); [Wang et al. \(2024b\)](#). Priority sampling methods are effective for handling network fluctuations, but they rely on stationary data distribution where bandwidth statistics (such as mean and variance) remain constant over time. These methods struggle with non-stationary scenarios where network conditions exhibit fundamental distribution shifts, such as abrupt changes in average bandwidth levels. On the other hand, meta-learning approaches, aim to learn from tasks with shared characteristics, but they require prior knowledge of network bandwidth patterns. However, obtaining such knowledge is inherently difficult due to the complex interplay of factors, including network traffic, geographical mobility, signal interference, and wireless channel dynamics.

In contrast to existing approaches that rely on prior knowledge of network bandwidth [Bentaleb et al. \(2024\)](#); [Patel et al. \(2024\)](#); [Wang et al. \(2024b\)](#), we propose a novel perspective for tackling non-stationary network resource adaptation: neural network plasticity. To the best of our knowledge, this is the first paper to analyze the optimization problem in non-stationary networks from the perspective of neural plasticity. Similar to biological neural systems [Puderbaugh and Emmady \(2023\)](#), artificial neural networks can experience plasticity degradation in non-stationary environments [Dohare et al. \(2024\)](#), where certain neurons become inactive and fail to adapt to fluctuations in network bandwidth. While this phenomenon of plasticity loss has been well-documented [Gulcehre et al. \(2022\)](#); [Lee et al. \(2024\)](#); [Lyle et al. \(2023\)](#), its underlying mechanisms are still poorly understood. Previous studies have identified dormant neurons with zero output as dormant neurons and linked them to plasticity loss [Sokar et al. \(2023\)](#). However, we argue that this characterization, based solely on forward propagation, oversimplifies the complex nature of neural plasticity in non-stationary environments.

In this paper, we propose a novel dual-zero criterion for identifying inactive neurons by examining both forward propagation and gradient values. Our key insight is that neural inactivity can only be conclusively determined when a neuron exhibits both zero forward propagation and zero gradients during backpropagation, indicating complete non-participation in both information flow and learning processes. This distinction is crucial: a neuron with zero forward propagation may still actively participate in learning through non-zero gradients, while a neuron with zero gradients but non-zero forward propagation continues to contribute to information propagation. This rigorous characterization leads to a novel theoretical framework for analyzing neural plasticity loss through the lens of forward and backward propagation in optimization. We formalize the concept of Silent Neurons - neurons exhibiting simultaneous zero forward propagation and zero gradients - and establish their relationship to plasticity degradation in non-stationary environments. Based on this theoretical foundation, we develop Reset Silent Neuron (ReSiN), a method that systematically identifies and reactivates Silent Neurons to maintain neural plasticity. Through extensive experiments analyzing neural network dynamics, we validate both our theoretical analysis and the effectiveness of ReSiN. The results demonstrate that ReSiN not only preserves neural plasticity but also achieves significant performance improvements in non-stationary network resource adaptation scenarios.

What we aim to optimize is the ability of a method to quickly learn and adapt when the data distribution changes rapidly, so that it can keep up with the evolving patterns. Although reinforcement learning has emerged as a popular solution for network resource allocation problems, it has yet to see widespread deployment in practice. A major reason is the discrepancy between training and deployment environments, which undermines the robustness of learned policies. This paper offers a new perspective on enabling rapid adaptation to such discrepancies. Our primary focus is on non-stationary network environments, our method demonstrates consistent performance improvements across both stationary and non-stationary scenarios. Our key contributions are:

- **Novel Problem Analysis:** We provide the first systematic analysis of network resource adaptation in non-stationary environments through neural plasticity. Our analysis reveals how internal neural dynamics directly impact adaptation capabilities, offering new insights into this fundamental networking challenge.
- **Theoretical Foundation:** We establish a rigorous theoretical framework that characterizes the intricate relationship between forward and backward propagation in neural plasticity loss. This framework formally defines Silent Neurons and proves that both propagation mechanisms must be jointly considered to fully characterize the necessary conditions for plasticity loss in deep neural networks.
- **Algorithm Design:** Based on our theoretical insights, we have developed Reset Silent Neuron (ReSiN), a practical method for detecting and reactivating Silent Neurons. This approach allows for continuous learning without the need for prior knowledge of network conditions or environmental characteristics.

- **Implementation and Evaluation:** Through extensive experiments in adaptive video streaming, we demonstrate that ReSiN achieves significant performance improvements over existing approaches. Our evaluation uses standardized metrics, fixed hyperparameters, and consistent random seeds to ensure reproducibility and fair comparison.

The rest of this paper is organized as follows: §2 presents the background of our work and motivates the research problems we address. §3 formulates the problem using stochastic adaptive video streaming as a case study. §4 presents our theoretical analysis of Silent Neurons and our proposed ReSiN method. §5 provides a comprehensive experimental evaluation. §6 discusses relevant literature and contextualizes our contributions. §7 concludes with future research directions.

## 2 Background and Motivation

In this section, we will first examine how non-stationarity fundamentally challenges the MDP formulation of network resource adaptation. Through empirical evaluation of adaptive video streaming, we will demonstrate how these challenges manifest in practice. We will then conduct a neuron-level analysis to identify the root cause of adaptation failure in neural networks. Based on these insights, we will present our solution that maintains learning capability under non-stationary conditions.

### 2.1 Non-stationary MDP

RL offers a promising approach to adapting network resources by utilizing Markov Decision Processes (MDPs) to model uncertainties. In an MDP, network scenarios and adaptation decisions are represented as states and actions, respectively. Formally, an MDP is defined by a tuple  $(\mathcal{S}, \mathcal{A}, \mathcal{P}, \mathcal{R}, \gamma)$ . The state space  $\mathcal{S}$  encompasses all possible network situations, while the action space  $\mathcal{A}$  includes all available adaptation decisions. The state transition function  $\mathcal{P} : \mathcal{S} \times \mathcal{A} \rightarrow \Delta(\mathcal{S})$  describes the dynamics of the environment, where  $\Delta(\mathcal{S})$  denotes the space of probability distributions over  $\mathcal{S}$ . Specifically, at time step  $t$ , given the current state  $s_t$  and action  $a_t$ , the probability of transitioning to the next state  $s_{t+1}$  is defined as  $p(s_{t+1} | s_t, a_t)$ . The reward function  $\mathcal{R} : \mathcal{S} \times \mathcal{A} \rightarrow \mathbb{R}$  provides immediate feedback  $r(s_t, a_t)$ , while the discount factor  $\gamma \in [0, 1)$  balances immediate and future rewards.

While this MDP formulation naturally captures bandwidth variations within a single network through transition probabilities  $p(s_{t+1} | s_t, a_t)$ , it fails to address the fundamental non-stationarity in modern networks. Common scenarios such as switching between 4G and WiFi, transitioning from cellular to tunnel environments, or roaming between carriers introduce structural changes in network characteristics. These changes manifest as shifts in both transition dynamics  $\mathcal{P}$  and reward structure  $\mathcal{R}$ , effectively creating transitions between different MDPs  $\{M_1, M_2, \dots, M_N\}$ , where each  $M_n = (\mathcal{S}, \mathcal{A}, \mathcal{P}_n, \mathcal{R}_n, \gamma)$  represents a distinct network environment. This non-stationarity fundamentally challenges learning algorithms, as policies optimized for one network environment can fail dramatically in another.

### 2.2 Impact of Non-stationarity on RL

To demonstrate the impact of non-stationarity on optimization algorithms, we conducted a systematic study using adaptive video streaming as our test scenario. This choice was made because adaptive video streaming presents the key challenges in network resource adaptation, such as real-time decision-making, direct impact on user experience, and complex trade-offs between quality and stability. We evaluated Proximal Policy Optimization (PPO), a state-of-the-art reinforcement learning algorithm known for its stability and sample efficiency, under three network conditions: high bandwidth (HBW), low bandwidth (LBW), and non-stationary (NS) environments. In the NS environment, we periodically alternated between HBW and LBW to simulate common network transitions. Figure 1 illustrates the algorithm’s performance deterioration under non-stationary conditions.

Results in Figure 1 reveal a critical limitation of PPO Agent under non-stationary conditions. When transitioning from HBW to LBW, the agent fails to match the performance baseline established in consistent LBW environments. More significantly, upon returning to HBW conditions, the agent cannot recover its original performance level, despite having previously optimized for this exact environment. This performance degradation persists even though the network merely

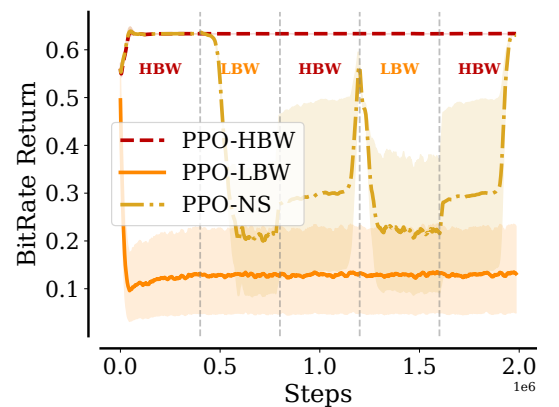


Figure 1: Performance comparison of bitrate returns in adaptive video streaming achieved by PPO under different bandwidth conditions.

cycles through previously encountered conditions (HBW  $\rightarrow$  LBW  $\rightarrow$  HBW), indicating that PPO loses its adaptation capability after experiencing non-stationarity. An intuitive and informal explanation for why PPO may struggle to adapt quickly in non-stationary environments is that the neural network becomes specialized in a particular data pattern. When the data distribution shifts, the agent must rapidly adjust its parameters to fit the new dynamics.

### 2.3 Neural Plasticity and Its Loss

The non-stationarity of network environments presents significant challenges for learning algorithms. Policies that are optimized for one environment may not perform well in another, requiring continuous adaptation by the learning agent. This need for continuous adaptation naturally leads us to consider neural plasticity - the ability of neural networks to modify their structure and parameters in response to changes in the environment. While neural plasticity is crucial for maintaining performance across varying conditions, it is often lost during training. Previous studies have primarily focused on characterizing this plasticity loss through dormant neurons - those with zero outputs in the forward pass Sokar et al. (2023); Xu et al. (2024). These dormant neurons become inactive and fail to contribute to the network’s adaptive capabilities.

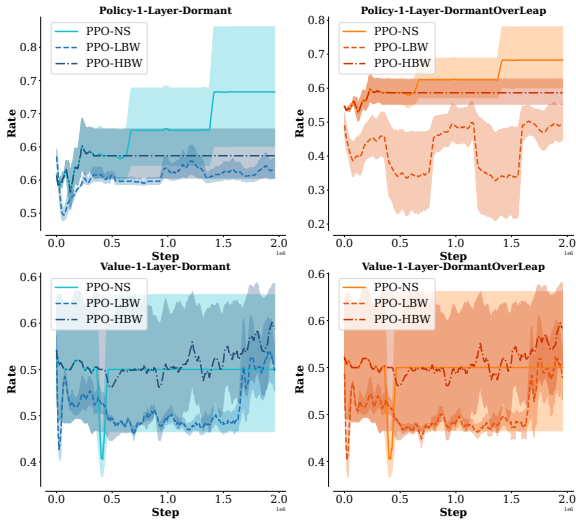


Figure 2: Evolution of neural network plasticity loss.

Figure 2 reveals widespread neuron inactivity during training, particularly pronounced under non-stationary conditions. The overlap coefficient (formally defined in Definition 2.1) demonstrates that once neurons become inactive, they remain dormant across subsequent time steps, indicating a systematic and persistent loss of neural plasticity.

**Definition 2.1 (Overlap Coefficient for Neuron).** *The overlap coefficient measures the similarity between the set of dormant or zero gradient neurons in each layer of a neural network at the current iteration and last iteration Sokar et al. (2023). Let  $A$  represent the set of dormant neurons at the current iteration, and  $B$  represent the set of dormant and zero gradient neurons at the previous iteration. The overlap coefficient between  $A$  and  $B$  is defined as follows:*

$$\text{overlap}(A, B) = \frac{|A \cap B|}{\min(|A|, |B|)}, \quad (2.1)$$

*This metric is used to measure the proportion of neurons that remain consistent over time, providing insights into the network’s insight state.*

However, we argue that this characterization is incomplete, as it overlooks the backward pass dynamics that are essential for learning and adaptation. Our analysis reveals that true plasticity loss occurs only when neurons exhibit both zero outputs in the forward pass and zero gradients in the backward pass, a condition we term as “Silent Neurons”. This dual-zero state indicates a complete disconnection from both information propagation and learning processes.

## 3 Network Resource Adaptation Problem

In this section, we will use adaptive video streaming as our representative case study for non-stationary network resource adaptation. Our mathematical model incorporates important practical factors such as network dynamics based on real-world trace files, transmission delays, and jitter. To accurately reflect user sensitivity to bitrate variations, we have chosen a non-convex QoE metric as the optimization objective for our reinforcement learning agent.

### 3.1 Stochastic Adaptive Video Streaming

Following the adaptive video streaming model Yin et al. (2015), a video is divided into  $I$  consecutive chunks  $\{V_1, V_2, \dots, V_I\}$ , each with a duration of  $t_i$ -seconds. Each chunk is encoded at multiple bitrate levels  $b \in \mathbb{B}$ , where  $\mathbb{B} = \{b_1, b_2, \dots, b_M\}$  represents the available bitrates in ascending order. The size of chunk  $i$  encoded at bitrate  $b$  is denoted as  $d_i(V_i^b)$ , which increases monotonically with  $b$ . The task of the reinforcement learning agent is to select the optimal bitrate for each chunk in order to maximize the quality of the streaming experience. To prevent interruptions during bitrate transitions between segments  $V_i$  and  $V_{i+1}$ , we implement a playback buffer  $B_f$ . This buffer pre-caches upcoming segments, allowing for concurrent video playback and segment downloading. The buffer occupancy  $B_f(t)$  is limited to the range of  $[0, B_f^{max}]$ , where  $B_f^{max}$  is determined by server policies or client storage constraints. However, network

bandwidth is non-stationary and exhibits shifting mean and variance, which presents significant challenges for adaptive streaming. Our optimization objective takes into account three key factors: maximizing video quality by selecting higher bitrates during stable periods, minimizing playback interruptions, and maintaining quality stability by avoiding frequent bitrate switches that can degrade the user experience.

The download time for segment  $V_i^b$  consists of the network round-trip time  $t_{RTT}$  and the data transfer time  $d_i(V_i^b)/S_i$ , where  $S_i$  represents the download speed. To reflect network variability, we incorporate a multiplicative noise factor in the relationship between consecutive segment start download times in Eq. (3.1)

$$t_{i+1}^d = t_i^d + \left( \frac{d_i(V_i^b)}{S_i} + t_{RTT} \right) \times \eta(i) + \Delta t_i^w, \quad (3.1)$$

where  $\eta(i)$  captures network variability and  $\Delta t_i^w$  represents intentional waiting time for buffer management. We define the total network delay as  $t_{delay} = \left( \frac{d_i(V_i^b)}{S_i} + t_{RTT} \right) \times \eta(i)$ .

The effective throughput, denoted as  $C_{t_i}$ , is calculated by taking the average download speed and excluding any waiting periods:

$$C_{t_i} = \frac{1}{t_{i+1}^d - t_i^d - \Delta t_i^w} \int_{t_i^d}^{t_{i+1}^d - \Delta t_i^w} S_t dt. \quad (3.2)$$

Buffer occupancy evolution captures the interplay between content downloading and playback. When a chunk of content, denoted as  $V_i$ , is successfully downloaded, it adds  $t_i$  seconds to the buffer. This results in the following dynamics:

$$B_f(t_{i+1}) = \left( (B_f(t_i) - t_{delay})_+ + t_i - \Delta t_i^w \right)_+. \quad (3.3)$$

Where  $(x)_+$  represents the non-negative operator  $\max(0, x)$ . This formulation addresses two critical buffer states: underflow and overflow. Buffer underflow occurs when  $B_f(t_i) < t_{delay}$ , which can result in playback interruption. To prevent buffer overflow, the player implements a waiting period:

$$\Delta t_i^w = \left( (B_f(t_i) - t_{delay})_+ + t_i - B_f^{max} \right)_+. \quad (3.4)$$

This mechanism maintains buffer occupancy below  $B_f^{max}$  while ensuring efficient resource utilization and smooth playback.

### 3.2 Object Function

In adaptive video streaming systems, optimizing Quality of Experience (QoE) remains a fundamental challenge. We formulate the QoE optimization problem by incorporating multiple critical metrics that impact user satisfaction. The primary component quantifies the average video quality across all chunks, expressed as  $\frac{1}{I} \sum_{i=1}^I q(V_i^b)$ , where  $q(\cdot)$  represents a monotonically non-decreasing quality assessment function. To account for the perceptual impact of quality fluctuations, we introduce a quality variation penalty term  $\frac{1}{I-1} \sum_{i=1}^{I-1} |q(V_{i+1}^b) - q(V_i^b)|$ , which captures the temporal quality dynamics between adjacent chunks. Our model also considers a key temporal factor that significantly influences user engagement: playback interruptions, which occur when buffer depletion leads to stalling events. We propose a comprehensive QoE metric that combines these components through a weighted sum formulation, enabling systematic optimization of the streaming strategy while balancing the inherent trade-offs among these competing objectives,

$$\begin{aligned} QoE_1^I &= \sum_{i=1}^I q(V_i^b) - \mu_1 \sum_{i=1}^{I-1} |q(V_{i+1}^b) - q(V_i^b)| \\ &\quad - \mu_2 \sum_{i=1}^I \left( \left( \frac{d_i(V_i^b)}{S_i} + t_{RTT} \right) \times \eta(i) - B_f(t_i) \right)_+. \end{aligned} \quad (3.5)$$

The composite QoE metric is defined by two weighting coefficients  $\mu_1$  and  $\mu_2$ , which allow for precise adjustment of the importance of each QoE component. This formulation takes into account the competing goals of maximizing average quality, maintaining consistent quality levels, and minimizing playback disruptions. By using this multi-objective

optimization framework, we can systematically navigate the complex trade-off space in adaptive video streaming. This allows streaming algorithms to adapt their behavior according to specific deployment scenarios and user preferences.

To accurately model the non-linear characteristics of human visual perception, we propose a novel quality function that captures both the diminishing returns of increased bitrate and the potential negative impacts of excessive bitrate consumption. Previous research has shown that there is a non-linear relationship between user-perceived quality and video bitrate [Zimmer et al. \(2010\)](#), meaning that as bitrate increases, the perceived quality improvement becomes less significant. To account for this effect, we use the function  $\log(\alpha + b_i)$ , where  $b_i$  represents the bitrate of chunk  $i$ , and  $\alpha$  represents a constant parameter. Additionally, we incorporate a penalty term  $-\frac{\beta}{b_i}$  to consider the limitations of resource and potential performance degradation associated with high bitrate selection. the value of  $\beta$  determines the strength of the penalty. This results in our proposed quality function:

$$q(V_i^b) = \log(\alpha + b_i) - \frac{\beta}{b_i}. \quad (3.6)$$

In contrast to existing approaches that rely on linear or convex optimization frameworks [Huang et al. \(2021\)](#); [Li et al. \(2024a\)](#), our formulation explicitly acknowledges the inherent non-convexity of the quality-bitrate relationship. This more realistic modeling choice introduces additional computational challenges, but it better reflects the complex nature of video streaming optimization in practice. In summary, the problem can be expressed as follows:

$$\begin{aligned} & \max_{V_1, \dots, V_I, t_s} \sum_{i=1}^I q(V_i^b) - \mu_1 \sum_{i=1}^{I-1} |q(V_{i+1}^b) - q(V_i^b)| \\ & - \mu_2 \sum_{i=1}^I \left( \left( \frac{d_i(V_i^b)}{S_i} + t_{RTT} \right) \times \eta(i) - B_f(t_i) \right)_+ \\ \text{st. } & t_{i+1}^d = t_i^d + \left( \frac{d_i(V_i^b)}{S_i} + t_{RTT} \right) \times \eta(i) + \Delta t_i^w \\ & C_t = \frac{1}{t_{i+1}^d - t_i^d - \Delta t_i^w} \int_{t_i^d}^{t_{i+1}^d - \Delta t_i^w} S_t dt \\ & B_f(t_{i+1}) = \left( (B_f(t_i) - t_{\text{delay}})_+ + t_i - \Delta t_i^w \right)_+ \\ & q(V_i^b) = \log(\alpha + b_i) - \frac{\beta}{b_i} \\ & B_f(t_i) \in [0, B_f^{\max}] \\ & b_i \in \mathbb{B}, \quad \forall i = 1, \dots, I \\ & \eta(i) \sim \mathcal{U}(0.9, 1.1). \end{aligned} \quad (3.7)$$

The complexity of this optimization problem arises from several key factors: (1) the incorporation of nonlinear network dynamics, (2) stochastic network variations modeled through multiplicative noise  $\eta(i) \sim \mathcal{U}(0.9, 1.1)$ , and (3) recursive buffer state evolution that captures temporal dependencies in streaming decisions. The difficulty of the problem is further compounded by the non-convex nature of our quality function  $q(V_i^b)$  and physical system constraints, such as the maximum buffer capacity  $B_f^{\max}$ . This combination of nonlinear dynamics, stochastic elements, and temporal dependencies results in a highly non-convex optimization landscape that closely mirrors the challenges faced by real-world adaptive streaming systems.

Given the complexity of the problem, we have chosen to use deep reinforcement learning (DRL) as our solution approach. To formulate the problem within the MDP framework, we have carefully designed the state space, action space, and reward function to accurately capture the dynamics of adaptive video streaming. Our state space, denoted as  $\mathcal{S}$ , includes key system parameters that influence streaming decisions such as the quality level of the previously downloaded chunk, current buffer occupancy, observed network throughput, network delay measurements, size information of pending video chunks, and the remaining number of chunks to be downloaded. This comprehensive representation of the state allows our DRL agent to make informed decisions based on both past performance and future streaming requirements. The action space, denoted as  $\mathcal{A}$ , consists of six discrete bitrate levels, each corresponding to a different quality representation for the video chunk. Our reward function has been carefully crafted to align with the objective of maximizing QoE, taking into account the complex interplay between maximizing video quality, minimizing quality variation, and preventing stalls.

## 4 Silent Neurons: Detection, Analysis and Reset Strategy

While the underlying mechanisms of plasticity loss remain an open research question, this section presents a systematic investigation into the role of dormant neurons - a widely adopted metric associated with plasticity degradation. We first examine the theoretical foundations and limitations of existing dormant neuron metrics. Building upon these insights, we introduce the concept of Silent Neurons and propose a novel methodology to mitigate plasticity loss through targeted intervention of Silent Neuron dynamics.

### 4.1 Dormant Neuron: Theoretical Analysis and Characterization

Consider a feed-forward neural network layer  $l$  characterized by its input space  $\mathcal{X}_l \subseteq \mathbb{R}^{k_l}$ , parameterized by  $\mathbf{W}_l \in \mathbb{R}^{k_{l+1} \times k_l}$  and  $\mathbf{b}_l \in \mathbb{R}^{k_{l+1}}$ , and with an activation function  $\sigma_l : \mathbb{R} \rightarrow \mathbb{R}$  applied elementwise. The forward pass of layer  $l$  is  $f_l(\mathbf{x}) = \sigma_l(\mathbf{W}_l \mathbf{x} + \mathbf{b}_l)$ , and the output of the  $i$ -th neuron in layer  $l$  is  $h_{l,i}(\mathbf{x}) = \sigma_l(\mathbf{w}_{l,i}^T \mathbf{x} + b_{l,i})$ , where  $\mathbf{w}_{l,i}^T$  is the  $i$ -th row of  $\mathbf{W}_l$ . Based on previous research [Sokar et al. \(2023\)](#); [Xu et al. \(2024\)](#), the dormant neuron can be defined in Definition 4.1.

**Definition 4.1 (Dormant Neuron).** For a layer  $l$  with  $H_l$  neurons, we define the dormancy index  $s_{l,i}$  of neuron  $(l, i)$  as:

$$s_{l,i} = \frac{\mathbb{E}_{\mathbf{x} \in D} |h_{l,i}(\mathbf{x})|}{\frac{1}{H_l} \sum_{j \in h} \mathbb{E}_{\mathbf{x} \in D} |h_{l,j}(\mathbf{x})|} \quad (4.1)$$

where  $\mathbb{E}_{\mathbf{x} \in D}$  represents expectation over inputs  $\mathbf{x}$  drawn from distribution  $D$ .

To establish the theoretical properties of dormant neurons, we introduce three key assumptions:

**Assumption 1 (Continuity and Differentiability).** The neuron output  $h_{l,j}(\mathbf{x})$  is continuously differentiable with respect to  $\mathbf{x}$ :  $h_{l,j} \in C^1(\mathbb{R}^{k_l})$ .

**Assumption 2 (Boundedness).** There exists  $M > 0$  such that  $\mathbb{E}_{\mathbf{x} \in D} |h_{l,j}(\mathbf{x})| \leq M$  for all  $j \in h$ .

**Assumption 3 (Non-degeneracy).** There exists  $m > 0$  such that  $\frac{1}{H_l} \sum_{j \in h} \mathbb{E}_{\mathbf{x} \in D} |h_{l,j}(\mathbf{x})| \geq m$ , ensuring a strictly positive denominator in the dormancy index.

These assumptions enable us to establish a fundamental property of dormant neurons:

**Lemma 4.1 (Forward Dormancy Lemma).** If  $s_{l,i} = 0$ , then  $h_{l,i}(\mathbf{x}) = 0$  for all  $\mathbf{x} \in D$ .

*Proof.* See Appendix A. □

**Lemma 4.2 (Forward-to-Backward Dormancy Lemma).** If  $s_{l,i} = 0$ , then  $\Delta h_{l,i}(\mathbf{x}) = 0$  for all  $\mathbf{x} \in D$ .

*Proof.* See Appendix B. □

**Lemma 4.3 (Backward Dormancy Lemma).** Suppose the gradient  $\nabla h_{l,i}(\mathbf{x}) = 0$  for all  $\mathbf{x} \in \mathcal{X}_l$ . Then  $h_{l,i}(\mathbf{x})$  is constant on  $\mathcal{X}_l$ . Moreover, if  $h_{l,i}(\mathbf{x}) = 0$  at any point  $\mathbf{x}_0 \in \mathcal{X}_l$ , then  $h_{l,i}(\mathbf{x}) = 0$  for all  $\mathbf{x} \in \mathcal{X}_l$ , and hence the neuron is dormant ( $s_{l,i} = 0$ ).

*Proof.* See Appendix C. □

These lemmas collectively unveil the intrinsic properties of dormant neurons from complementary perspectives. Building upon these foundational results, we present a comprehensive characterization of bidirectional dormancy in Theorem 4.4, which provides a unified framework for analyzing neural network plasticity.

**Theorem 4.4 (Bidirectional Dormancy Characterization).** Let  $D \subseteq \mathcal{X}_l \subseteq \mathbb{R}^{k_l}$  be the domain from which inputs  $\mathbf{x}$  are drawn. Consider layer  $l$  with  $H_l$  neurons. For the  $i$ -th neuron in layer  $l$ , let

$$h_{l,i}(\mathbf{x}) = \sigma_l(\mathbf{w}_{l,i}^T \mathbf{x} + b_{l,i}), \quad (4.2)$$

where  $\sigma_l$  is continuously differentiable and applied elementwise. The neuron's dormancy index is defined as:

$$s_{l,i} = \frac{\mathbb{E}_{\mathbf{x} \in D} |h_{l,i}(\mathbf{x})|}{\frac{1}{H_l} \sum_{j=1}^{H_l} \mathbb{E}_{\mathbf{x} \in D} |h_{l,j}(\mathbf{x})|} \quad (4.3)$$

Assume:

1. (Continuity and Differentiability)  $h_{l,i}(\mathbf{x})$  is in  $C^1(\mathbb{R}^{k_l})$ .

2. (Boundedness)  $\exists M > 0: \mathbb{E}_{\mathbf{x} \in D} |h_{l,i}(\mathbf{x})| \leq M$ .
3. (Non-degeneracy)  $\exists m > 0: \frac{1}{H_l} \sum_{j=1}^{H_l} \mathbb{E}_{\mathbf{x} \in D} |h_{l,j}(\mathbf{x})| \geq m$ .

Then the following two statements are equivalent:

- (A) Dormancy:  $s_{l,i} = 0$ . Equivalently,  $\mathbb{E}_{\mathbf{x} \in D} |h_{l,i}(\mathbf{x})| = 0$ .
- (B) Zero Gradient (on  $D$ ) plus at least one zero activation:

$$\nabla h_{l,i}(\mathbf{x}) = 0 \quad \forall \mathbf{x} \in D \quad \text{and} \quad \exists \mathbf{x}_0 \in D : h_{l,i}(\mathbf{x}_0) = 0. \quad (4.4)$$

*Proof.* See Appendix D. □

Our theoretical analysis highlights the valuable insights that dormant neurons can provide in understanding plasticity loss. However, there are several important limitations that should be addressed. Firstly, the characterization of dormant neurons heavily relies on the choice of input distribution  $D$ . This means that different distributions may lead to varying conclusions about the presence of dormant neurons. Secondly, the zero-activation condition (B) is only required to hold over the distribution  $D$ , rather than the entire input space  $\mathcal{X}_l$ . This could potentially limit the robustness of detecting dormancy. Additionally, in practical implementations, dormant neurons are typically identified when their dormancy index  $s_{l,i}$  falls below a small threshold  $\epsilon$ , rather than requiring exact zero values. This introduces additional complexity to the theoretical guarantees.

## 4.2 Silent Neurons and Reset Mechanism

While the Dormant Neuron metric characterizes neural inactivity through forward propagation behavior, its implications for backward propagation require restrictive conditions. To address these limitations and provide a more comprehensive analysis of neural network dynamics, we propose an approach that directly examines gradient behavior in response to network inputs:

$$g_\theta = \nabla_\theta \sum_i f_\theta(s_i). \quad (4.5)$$

Where  $f_\theta$  represents the neural network function and  $s_i$  represents input states from a batch, this formulation offers three key advantages over traditional approaches. Our loss-independent analysis directly examines the network's response to inputs, avoiding the potential masking of neuron activity that can occur with loss-based gradients where neurons may be active in forward propagation despite zero gradients. By aggregating gradients across all outputs ( $\sum_i f_\theta(s_i)$ ), we achieve comprehensive activation assessment that captures the complete spectrum of neuron contributions across the decision space. This transcends the limitations of specific optimization objectives. Furthermore, this approach ensures thorough state-space coverage, enabling the detection of neurons critical for particular state representations that may not be directly reflected in the current loss function. This is a crucial consideration in non-stationary environments where neuron importance may vary across different operating conditions. Based on this analysis, we define Silent Neurons as follows:

**Definition 4.2 (Silent Neuron).** Let  $H_l$  be the number of neurons in layer  $l$ . The activity index  $\xi_{l,i}$  for neuron  $(l, i)$  is defined by both its forward output and backward gradient:

$$\xi_{l,i} = \frac{\mathbb{E}_{\mathbf{x} \in D} |h_{l,i}(\mathbf{x})| \cdot \mathbb{E}_{\mathbf{x} \in D} |g_{l,i}(\mathbf{x})|}{\frac{1}{H_l} \sum_{j \in h} (\mathbb{E}_{\mathbf{x} \in D} |h_{l,j}(\mathbf{x})|)} \quad (4.6)$$

where  $h_{l,i}(\mathbf{x})$  denotes the output of neuron  $(l, i)$  for input  $\mathbf{x}$ , and  $g_{l,i}(\mathbf{x}) = \frac{\partial}{\partial h_{l,i}} \sum_i f_\theta(\mathbf{x}_i)$  represents its gradient computed from the aggregated network outputs.

Building upon the formal characterization presented in Definition 4.2, we establish a fundamental theoretical result in Theorem 4.5 that provides comprehensive insights into the nature of silent neurons.

**Theorem 4.5 (Silent Neuron Characterization).** Let  $D \subseteq \mathcal{X}_l \subseteq \mathbb{R}^{k_l}$  be the domain from which inputs  $\mathbf{x}$  are drawn. Consider layer  $l$  with  $H_l$  neurons. For the  $i$ -th neuron in layer  $l$ , let

$$h_{l,i}(\mathbf{x}) = \sigma_l \left( \mathbf{w}_l, i^T \mathbf{x} + b_l, i \right), \quad (4.7)$$

where  $\sigma_l$  is continuously differentiable and applied elementwise. The neuron's activity index is defined as:

$$\xi_{l,i} = \frac{\mathbb{E}_{\mathbf{x} \in D} |h_{l,i}(\mathbf{x})| \cdot \mathbb{E}_{\mathbf{x} \in D} |g_{l,i}(\mathbf{x})|}{\frac{1}{H_l} \sum_{j \in h} (\mathbb{E}_{\mathbf{x} \in D} |h_{l,j}(\mathbf{x})|)}, \quad (4.8)$$

where  $g_{l,i}(\mathbf{x}) = \frac{\partial}{\partial h_{l,i}} \sum_i f_\theta(\mathbf{x}_i)$  represents the neuron’s gradient computed from the aggregated network outputs. Assume:

1. (Continuity and Differentiability)  $h_{l,i}(\mathbf{x})$  and  $g_{l,i}(\mathbf{x})$  are in  $C^1(\mathbb{R}^{k_l})$ .
2. (Boundedness)  $\exists M_h, M_g > 0: \mathbb{E}_{\mathbf{x} \in D} |h_{l,i}(\mathbf{x})| \leq M_h$  and  $\mathbb{E}_{\mathbf{x} \in D} |g_{l,i}(\mathbf{x})| \leq M_g$ .
3. (Non-degeneracy)  $\exists m > 0: \frac{1}{H_l} \sum_{j=1}^{H_l} \mathbb{E}_{\mathbf{x} \in D} |h_{l,j}(\mathbf{x})| \geq m$ .

Then for an arbitrarily small constant  $\epsilon > 0$ , the following statements are equivalent:

- (A) Silence:  $\sigma_{l,i} < \epsilon$ .
- (B) Zero Forward and Backward Activity (on  $D$ ):

$$\mathbb{E}_{\mathbf{x} \in D} |h_{l,i}(\mathbf{x})| < \sqrt{\epsilon} \quad \text{and} \quad \mathbb{E}_{\mathbf{x} \in D} |g_{l,i}(\mathbf{x})| < \sqrt{\epsilon}. \quad (4.9)$$

*Proof.* See Appendix E □

Theorem 4.5 enhances our comprehension of neural network behavior by addressing the main shortcomings in characterizing dormant neurons. The traditional dormancy condition,  $s_{l,i} = 0$ , implies that a neuron’s expected output,  $\mathbb{E}_{\mathbf{x} \in D} |h_{l,i}(\mathbf{x})| = 0$ , must be exactly zero over distribution  $D$  if the gradient is also zero. However, our proposed Silent Neuron framework introduces a more nuanced and practical approach.

The Silent Neuron characterization utilizes the activity index  $\xi_{l,i}$ , which takes into account both forward and backward propagation patterns across the input distribution  $D$ . Instead of strictly enforcing zero conditions, we introduce a threshold-based criterion  $\xi_{l,i} < \epsilon$  that allows for near-zero activities. This relaxation offers two significant advantages: (1) it better reflects real-world scenarios where exact zero activities are unlikely, and (2) it improves robustness across varying input distributions by focusing on consistently low activity patterns rather than exact zeros. (If we were to relax the dormancy criterion to  $s_{l,i} < \epsilon$ , it would fundamentally prevent the derivation of gradient-based properties.)

Silent neurons, characterized by minimal forward and backward activity, effectively represent units with limited plasticity in the network. Their negligible contribution to both computation and gradient-based learning makes them strong candidates for reset operations. Consequently, our Reset Silent Neuron methodology implements a straightforward yet effective reset criterion: when  $\xi_{l,i} < \epsilon$ , the corresponding neuron is reset to restore its learning potential. The process of ReSiN is shown in Algorithm 1.

## 5 Experiments

We are conducting experiments to address the following key questions: 1) How does system behavior evolve under non-stationary environments? 2) Is the loss of neural plasticity a verifiable phenomenon? 3) Can our Silent Neuron reset method effectively maintain plasticity and outperform dormant reset? 4) Does bidirectional propagation loss monitoring enable better reset strategies than unidirectional approaches? 5) Does our approach demonstrate robustness at both the local level (under different reset thresholds) and the global level (across the entire algorithmic framework)? (The comprehensive ablation studies presented in Appendix G validate the robustness of our algorithmic design.)

### 5.1 Experiment Setting

All code and data will be open-sourced upon paper acceptance. Experimental settings remain consistent across evaluations, including random seeds, with variations only in method implementations and necessary non-stationary transitions.

### 5.2 Non-stationarity System Analysis

What is the state of the entire system during periods of non-stationarity? As shown in Figure 1, the PPO algorithm experiences significant performance decline in non-stationary environments, struggling to effectively adjust to changes in the environment. To gain a better understanding of this phenomenon, we analyze the internal states of the neural networks by examining both individual reward and system information metrics.

Figure 3 illustrates the significant impact of non-stationarity on the learning system’s plasticity. The agent is unable to regain its pre-transition performance across all QoE metrics, indicating a persistent loss of adaptability. The agent shows poor adaptation during network transitions in both directions. When bandwidth decreases, it continues to select high bitrates despite reduced capacity. Conversely, when bandwidth increases, it fails to take advantage of the additional resources, resulting in low bitrates and a sudden surge in rebuffer time and reward. This bidirectional adaptation failure

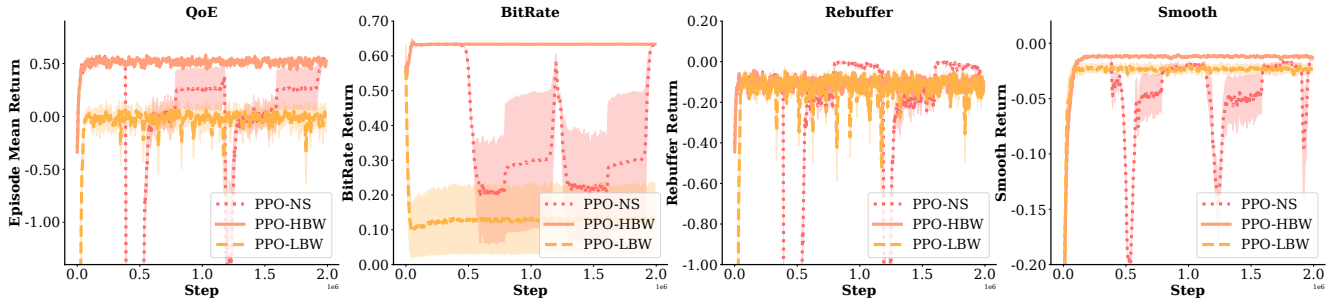


Figure 3: Performance comparison of PPO under different network conditions in terms of QoE metrics. The figure shows the learning curves of the total QoE reward and its components.

highlights the system’s state during periods of non-stationarity: a fundamental loss of plasticity, leaving the agent unable to effectively respond to dynamic network conditions. This rigidity leads to suboptimal performance and a degraded user experience.

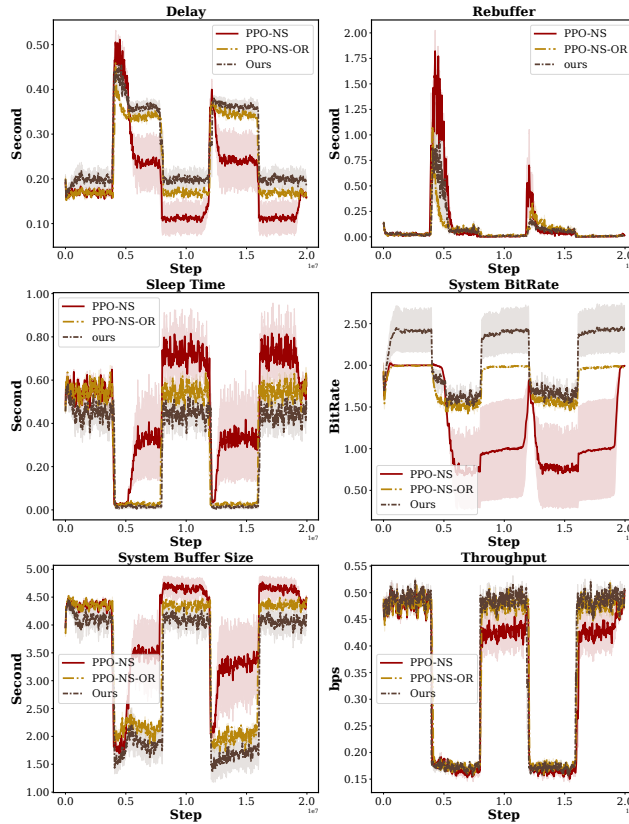


Figure 4: System metrics under different plasticity maintenance strategies in non-stationary environments are compared in the figure. The strategies include standard PPO (PPO-NS), PPO with output-based reset using dormant neuron detection (PPO-NS-OR), and our proposed method of PPO with intersection-based reset using the proposed Silent Neuron criterion (Ours).

Figure 4 reveals how non-stationarity affects system behavior and resource utilization. Network transitions trigger abrupt changes, notably in rebuffering duration. The agent struggles to adapt, leading to suboptimal resource utilization: excessive buffering, extended sleep intervals, and underutilized throughput. This translates to degraded user experience, with the system exhibiting either over-conservative (excessive buffering and sleep time) or over-aggressive (increased rebuffering) behavior during transitions, indicating an inability to maintain optimal operation under changing conditions.

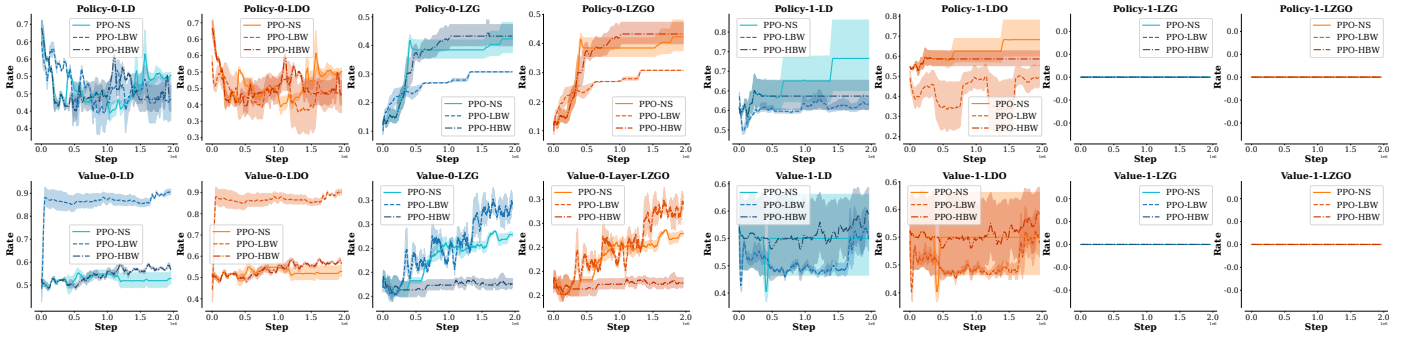


Figure 5: The activity patterns of neurons across network layers and components, such as the ratio of dormant neurons (Layer-Dormant, LD), the persistence of dormant neurons (DormantOverLeap, LDO), the ratio of zero gradients (ZeroGradient, LZG), and the persistence of zero gradients (ZeroGradientOverLeap, LZGO) are examined for both policy (Policy-0, Policy-1) and value (Value-0, Value-1) networks.

### 5.3 Neural Plasticity Loss and Adaptation Capability

In this section, we will analyze from the perspective of neuron outputs and gradients in order to understand why neural networks struggle to quickly adapt and learn in non-stationary environments. Figure 5 provides important insights into the loss of neural plasticity. It is evident from the figure that once neurons become dormant, they tend to remain inactive in subsequent iterations, as indicated by the overlap between the dormant neuron curves and their persistence metrics. This phenomenon can be described as a “plasticity trap”, where neurons lose their ability to adapt to new conditions in network resource adaptation tasks.

Figure 5 also illustrates an increasing proportion of dormant and zero-gradient neurons during training in non-stationary environments, indicating a progressive loss of plasticity. Interestingly, similar patterns emerge in both high and low bitrate scenarios, suggesting that plasticity loss is inherent in RL tasks where expected future reward distributions evolve and network conditions fluctuate. The analysis reveals layer-wise differences in plasticity loss: the shallow layer (Layer 0) shows more severe loss compared to the deeper layer (Layer 1) in both policy and value networks. This suggests that the network’s basic feature processing is more vulnerable to plasticity loss than higher-level processing in adaptive video streaming tasks.

The findings provide strong evidence that neural plasticity loss is a fundamental challenge in network resource adaptation, especially in non-stationary environments. The progressive and persistent nature of this loss explains why conventional approaches struggle to maintain performance under dynamic network conditions.

### 5.4 Performance Evaluation

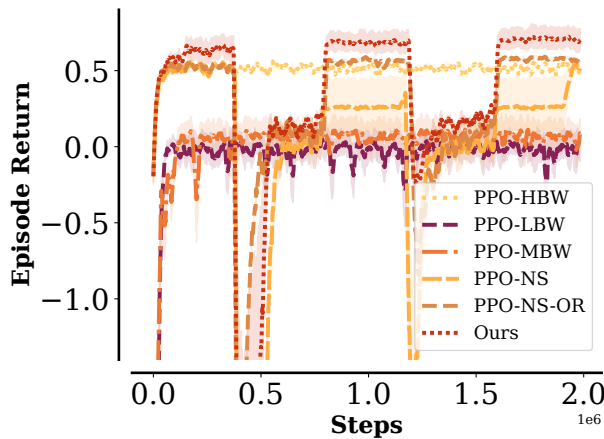


Figure 6: Performance comparison of PPO variants across different network conditions and plasticity maintenance strategies. The figure shows the learning curves of QoE rewards for six scenarios: PPO-HBW, PPO-LBW, PPO in mixed-bandwidth environments (PPO-MBW), PPO-NS, PPO-NS-OR, and Ours.

Figure 6 shows that our Silent Neuron reset method outperforms conventional approaches, addressing plasticity loss caused by both non-stationary network conditions and inherent RL processes. It surpasses the performance of the conventional approach in stable high-bandwidth conditions (PPO-HBW) and significantly outperforms the dormant-based reset method. These results highlight the importance of considering both forward outputs and backward gradients for robust adaptation in dynamic environments.

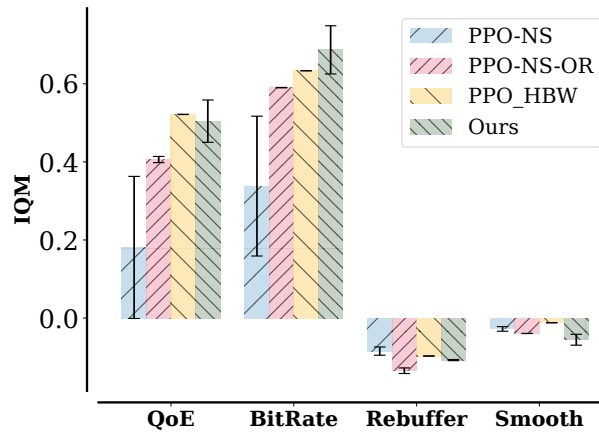


Figure 7: Comparison of QoE Methods using the IQM (Interquartile Mean) with a focus on the 25th-75th percentile returns. This approach aims to highlight the relative performance of different methods while minimizing the impact of outliers.

Further analysis of the reward components over time reveals the underlying mechanism of our method’s superior performance, as shown in Figure 7. Our Silent Neuron reset approach demonstrates a sophisticated balance in optimizing multiple QoE metrics simultaneously. Specifically, while maintaining low rebuffering events and ensuring smooth bitrate transitions, our method exhibits more aggressive yet stable bitrate selection behavior. This optimal trade-off is achieved through enhanced plasticity maintenance, allowing the agent to make more informed decisions without compromising system stability. This behavior is particularly noteworthy as it indicates that our method not only preserves adaptation capability but also enables more efficient exploration of the action space, resulting in improved user experience through higher video quality without sacrificing playback continuity.

### 5.5 Analysis of Neural Activity Patterns and Method Effectiveness

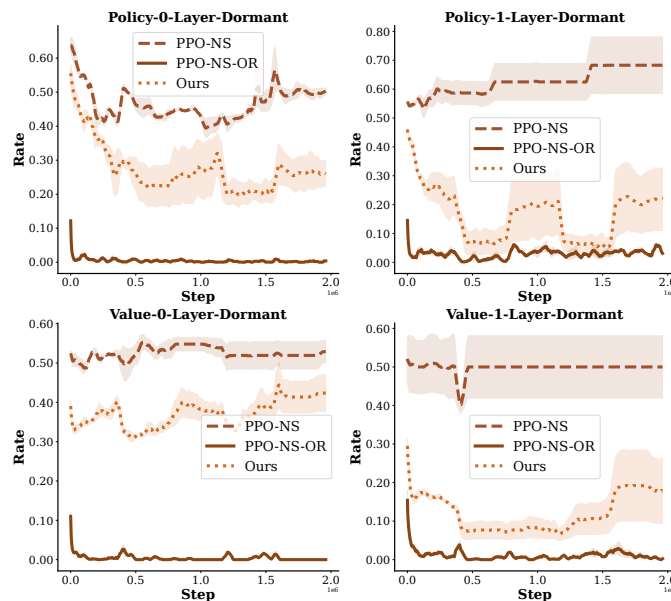


Figure 8: Dormancy patterns in policy and value networks, specifically in layers 0-1. It explores how plasticity maintenance strategies affect learning and neural dynamics.

Figure 8 illustrates that dormant neurons do not necessarily indicate a loss of plasticity. Our Silent Neuron reset method produces more dormant neurons compared to output reset, but it still achieves better performance in non-stationary environments. This supports our theory that neurons with zero outputs but non-zero gradients can improve network expressiveness and adaptability, challenging the traditional belief that dormant neurons lead to reduced plasticity. These empirical results provide evidence for our theoretical framework on neural plasticity in deep RL systems.

## 6 Related Work

This paper addresses the fundamental challenge of non-stationary network bandwidth in dynamic resource adaptation systems. We organize related work into three key areas: §6.1 examines existing approaches for handling network bandwidth variations, highlighting their limitations in non-stationary environments. §6.2 reviews optimization methods in adaptive video streaming, which serves as our driving application for studying non-stationary network resource adaptation. §6.3 surveys recent advances in plasticity-aware neural networks, particularly their capacity for maintaining adaptability in dynamic environments. Throughout our discussion, we emphasize how our proposed ReSiN method advances the state-of-the-art in each area by effectively maintaining neural plasticity under non-stationary conditions.

### 6.1 Non-stationary Environment

The challenge of non-stationary network environments presents fundamental difficulties for adaptive video streaming systems. While Plume addresses the imbalanced distribution of network bandwidth data through clustering and prioritized trace sampling [Patel et al. \(2024\)](#), this approach fails to fully capture the non-stationary nature of the problem within its reinforcement learning framework. By modeling a non-stationary problem within a stationary Markov Decision Process (MDP) framework, it encounters inherent limitations in handling truly dynamic network conditions. To address highly volatile network conditions, some approaches have turned to meta-reinforcement learning [Wang et al. \(2024b\)](#). Meta-learning strives to develop systems that can “learn how to learn” across multiple tasks [Li et al. \(2023\)](#), enabling rapid adaptation to new environments. However, while meta-learning enhances model generalization, it still relies on an underlying assumption that training tasks share certain stationary properties in their distributions. This makes it suboptimal for truly non-stationary environments where such assumptions may not hold. Alternative approaches like Self-Play Framework have shown promise in handling dynamic objective functions, though their application to network bandwidth optimization remains limited [Huang et al. \(2021\)](#); [Li et al. \(2024a\)](#).

A significant number of existing approaches combine bandwidth prediction with search algorithms to optimize video chunk selection [Lebreton and Yamagishi \(2024\)](#); [Wang et al. \(2024a\)](#); [Yin et al. \(2024\)](#). However, these methods’ heavy reliance on prediction accuracy becomes particularly problematic in non-stationary network environments, where the underlying bandwidth distribution experiences temporal shifts. The violation of the independently and identically distributed (i.i.d.) data assumption in non-stationary conditions fundamentally challenges these prediction-based approaches. As network dynamics evolve, models trained on historical data struggle to capture emerging patterns, resulting in suboptimal chunk selection decisions that ultimately degrade streaming quality.

### 6.2 Optimization Method

The challenge of optimizing video streaming systems has spawned diverse algorithmic approaches, each with distinct limitations in handling real-world complexity. Traditional optimization-based methods, while mathematically rigorous, require comprehensive knowledge of system dynamics and constraints [Spiteri et al. \(2020\)](#). Their computational complexity often renders them impractical for real-time decision-making scenarios. Similarly, dynamic programming approaches face inherent scalability limitations due to the curse-of-dimensionality, as their state space grows exponentially with system variables. These methods also depend heavily on accurate transition probability models between states, which are often difficult to obtain in practice. While Lyapunov control-based methods offer theoretical stability guarantees, their practical implementation is hindered by stringent assumptions about system dynamics and the complexity of optimizing control parameters.

Model Predictive Control (MPC) represents another significant approach, but its effectiveness is intrinsically tied to the accuracy of network bandwidth predictions [Lebreton and Yamagishi \(2022\)](#); [Lin and Wang \(2024\)](#). In non-stationary network environments, where bandwidth distributions experience temporal shifts, MPC faces substantial challenges. These out-of-distribution scenarios lead to significant deviations between predicted and actual bandwidth patterns, cascading into suboptimal control decisions that manifest as degraded QoE metrics, including increased latency and buffer underflows [Alomar et al. \(2023\)](#); [Yin et al. \(2015\)](#).

Recent innovations have attempted to address these limitations, such as the Two-Stage Deep Reinforcement Learning approach for 360-degree Video Streaming Scheduling, which incorporates an auxiliary agent for prediction error compensation [Bi et al. \(2024\)](#). However, this solution introduces its own challenges: significant computational overhead and an inflexible error correction mechanism that struggles to accommodate varying degrees of prediction discrepancies.

Furthermore, research has shown that sequential optimization of the two stages does not guarantee global optimality for the complete two-stage optimization problem He et al. (2025), highlighting the need for more sophisticated approaches that can handle the inherent complexity of video streaming optimization.

### 6.3 Neural Plasticity

Reinforcement learning systems demonstrate a marked tendency to lose plasticity when operating in non-stationary environments Dohare et al. (2024). Current research approaches this challenge through two distinct methodologies. The first focuses on preventive measures during the training process, employing specialized techniques such as distribution-regulating normalization methods Lyle et al. (2024a) and sophisticated weight constraint mechanisms. These mechanisms serve dual purposes: controlling parameter magnitudes and maintaining proximity to initial distributions Elsayed et al. (2024); Kumar et al. (2023).

The second methodology addresses networks that have already experienced plasticity loss through parameter resetting approaches Dohare et al. (2024); Juliani and Ash (2024); Liu et al. (2024). This category encompasses several innovative solutions, including Neuroplastic Expansion Liu et al. (2024), which enables incremental network growth through strategic neuron addition, and Continual Backpropagation Dohare et al. (2024), which employs systematic identification and reinitialization of underperforming neurons. Similarly, methods like ReDO Sokar et al. (2023) and Plasticity Injection Nikishin et al. (2024) maintain network adaptability through strategic neuron management during training. However, while these approaches offer practical solutions, they fall short of explaining the fundamental mechanisms driving plasticity loss Gulcehre et al. (2022); Lee et al. (2024); Lewandowski et al. (2024); Lyle et al. (2023, 2024b). To address this limitation, we propose a gradient-based metric for quantifying neuronal plasticity, providing a more nuanced and theoretically grounded framework for understanding network plasticity characteristics.

## 7 Conclusions and Future Work

This paper presents a comprehensive investigation of neural plasticity in network resource adaptation in non-stationary environments. The theoretical analysis explains the reason for the decline in network performance under non-stationary conditions, attributing it to a loss of plasticity. To address this issue, we propose the use of Silent Neurons, a novel metric that takes into account both forward outputs and backward gradients and develop a corresponding reset mechanism. Our experiments confirm the existence of plasticity loss and demonstrate the effectiveness of our solution. Interestingly, our findings also suggest that neurons with zero outputs but active gradients can actually improve network adaptability. Overall, our results showcase the superior performance of our approach in non-stationary network environments.

Looking forward, several promising directions emerge for future research. First, our framework could be extended to more complex scenarios where non-stationarity arises from various sources beyond network bandwidth, such as adversarial perturbations or user-induced variations. Second, while our Silent Neuron metric provides a more comprehensive measure of neural plasticity, investigating alternative or complementary indicators of plasticity could further enhance our understanding of neural network adaptation in dynamic environments. These extensions would contribute to developing more robust and adaptive systems for real-world applications.

## References

- A. Alomar, P. Hamadani, A. Nasr-Esfahany, A. Agarwal, M. Alizadeh, and D. Shah. Causalsim: A causal framework for unbiased trace-driven simulation. In M. Balakrishnan and M. Ghobadi, editors, *NSDI*, pages 1115–1147. USENIX Association, 2023.
- A. Bentaleb, M. Lim, M. N. Akcay, A. C. Begen, and R. Zimmermann. Bitrate adaptation and guidance with meta reinforcement learning. *IEEE Transactions on Mobile Computing*, 2024.
- S. Bi, H. Chen, X. Li, S. Wang, Y. Wu, and L. Qian. A two-stage deep reinforcement learning framework for mec-enabled adaptive 360-degree video streaming. *IEEE Transactions on Mobile Computing*, 2024.
- J. Cao, W. S. Cleveland, D. Lin, and D. X. Sun. On the nonstationarity of internet traffic. In M. K. Vernon, editor, *SIGMETRICS/Performance*, pages 102–112. ACM, 2001. ISBN 1-58113-334-0. URL <http://dblp.uni-trier.de/db/conf/sigmetrics/sigmetrics2001.html#CaoCLS01>.
- S. Deng, R. Netravali, A. Sivaraman, and H. Balakrishnan. Wifi, lte, or both? measuring multi-homed wireless internet performance. In *Proceedings of the 2014 Conference on Internet Measurement Conference*, pages 181–194, 2014.
- S. Dohare, J. F. Hernandez-Garcia, Q. Lan, P. Rahman, A. R. Mahmood, and R. S. Sutton. Loss of plasticity in deep continual learning. *Nature*, 632(8026):768–774, 2024.
- M. Elsayed, Q. Lan, C. Lyle, and A. R. Mahmood. Weight clipping for deep continual and reinforcement learning. *Reinforcement Learning Journal*, 5:2198–2217, 2024.

- C. Gulcehre, S. Srinivasan, J. Sygnowski, G. Ostrovski, M. Farajtabar, M. Hoffman, R. Pascanu, and A. Doucet. An empirical study of implicit regularization in deep offline RL. *Transactions on Machine Learning Research*, 2022. ISSN 2835-8856. URL <https://openreview.net/forum?id=HFfJWx60IT>.
- Z. He, W. Qiu, W. Zhao, X. Shao, and Z. Liu. Understanding world models through multi-step pruning policy via reinforcement learning. *Information Sciences*, 686:121361, 2025.
- P. Hu, Y. Chen, L. Pan, Z. Fang, F. Xiao, and L. Huang. Multi-user delay-constrained scheduling with deep recurrent reinforcement learning. *IEEE/ACM Transactions on Networking*, 2024.
- T. Huang, R.-X. Zhang, and L. Sun. Zwei: A self-play reinforcement learning framework for video transmission services. *IEEE Transactions on Multimedia*, 24:1350–1365, 2021.
- Y. Jia, C. Zhang, Y. Huang, and W. Zhang. Lyapunov optimization based mobile edge computing for internet of vehicles systems. *IEEE Transactions on Communications*, 70(11):7418–7433, 2022.
- A. Juliani and J. T. Ash. A study of plasticity loss in on-policy deep reinforcement learning. *arXiv preprint arXiv:2405.19153*, 2024.
- N. Kan, Y. Jiang, C. Li, W. Dai, J. Zou, and H. Xiong. Improving generalization for neural adaptive video streaming via meta reinforcement learning. In *Proceedings of the 30th ACM International Conference on Multimedia*, pages 3006–3016, 2022.
- S. Kumar, H. Marklund, and B. Van Roy. Maintaining plasticity in continual learning via regenerative regularization. 2023.
- P. Lebreton and K. Yamagishi. Adaptive bitrate control mechanism based on long-term evaluation. In *2022 IEEE International Conference on Multimedia and Expo (ICME)*, pages 01–06. IEEE, 2022.
- P. Lebreton and K. Yamagishi. Long-term adaptive bitrate control mechanism. *IEICE Transactions on Communications*, 107(11):817–830, 2024.
- H. Lee, H. Cho, H. Kim, D. Kim, D. Min, J. Choo, and C. Lyle. Slow and steady wins the race: Maintaining plasticity with hare and tortoise networks. In R. Salakhutdinov, Z. Kolter, K. Heller, A. Weller, N. Oliver, J. Scarlett, and F. Berkenkamp, editors, *Proceedings of the 41st International Conference on Machine Learning*, volume 235 of *Proceedings of Machine Learning Research*, pages 26416–26438. PMLR, 21–27 Jul 2024. URL <https://proceedings.mlr.press/v235/lee24d.html>.
- A. Lewandowski, H. Tanaka, D. Schuurmans, and M. C. Machado. Directions of curvature as an explanation for loss of plasticity, 2024. URL <https://arxiv.org/abs/2312.00246>.
- W. Li, X. Li, Y. Xu, Y. Yang, and S. Lu. Metaabr: A meta-learning approach on adaptive bitrate selection for video streaming. *IEEE Transactions on Mobile Computing*, 23(3):2422–2437, 2023.
- W. Li, J. Huang, Y. Liang, Q. Su, J. Liu, W. Lyu, and J. Wang. Optimizing video streaming in dynamic networks: An intelligent adaptive bitrate solution considering scene intricacy and data budget. *IEEE Transactions on Mobile Computing*, 2024a.
- W. Li, J. Huang, Q. Su, W. Jiang, and J. Wang. A learning-based approach for video streaming over fluctuating networks with limited playback buffers. *Computer Communications*, 214:113–122, 2024b.
- J. Lin and S. Wang. Adaptive video streaming in integrated satellite-terrestrial networks: A low-complexity model predictive control approach. *IEEE Wireless Communications Letters*, 2024.
- J. Liu, J. Obando-Ceron, A. Courville, and L. Pan. Neuroplastic expansion in deep reinforcement learning. *arXiv preprint arXiv:2410.07994*, 2024.
- Z. Liu, Q. Li, X. Chen, C. Wu, S. Ishihara, J. Li, and Y. Ji. Point cloud video streaming: Challenges and solutions. *IEEE Network*, 35(5):202–209, 2021.
- C. Lyle, Z. Zheng, E. Nikishin, B. A. Pires, R. Pascanu, and W. Dabney. Understanding plasticity in neural networks. In *ICML*, volume 202 of *Proceedings of Machine Learning Research*, pages 23190–23211. PMLR, 2023. URL <http://dblp.uni-trier.de/db/conf/icml/icml2023.html#LyleZNPPD23>.
- C. Lyle, Z. Zheng, K. Khetarpal, J. Martens, H. van Hasselt, R. Pascanu, and W. Dabney. Normalization and effective learning rates in reinforcement learning. In *The Thirty-eighth Annual Conference on Neural Information Processing Systems*, 2024a. URL <https://openreview.net/forum?id=ZbjJE6Nq5k>.
- C. Lyle, Z. Zheng, K. Khetarpal, H. van Hasselt, R. Pascanu, J. Martens, and W. Dabney. Disentangling the causes of plasticity loss in neural networks, 2024b. URL <https://arxiv.org/abs/2402.18762>.
- H. Mao, R. Netravali, and M. Alizadeh. Neural adaptive video streaming with pensieve. In *Proceedings of the conference of the ACM special interest group on data communication*, pages 197–210, 2017.
- Z. Meng, Y. Guo, Y. Shen, J. Chen, C. Zhou, M. Wang, J. Zhang, M. Xu, C. Sun, and H. Hu. Practically deploying heavyweight adaptive bitrate algorithms with teacher-student learning. *IEEE/ACM Transactions on Networking*, 29(2): 723–736, 2021.

- E. Nikishin, J. Oh, G. Ostrovski, C. Lyle, R. Pascanu, W. Dabney, and A. Barreto. Deep reinforcement learning with plasticity injection. *Advances in Neural Information Processing Systems*, 36, 2024.
- S. Padakandla. A survey of reinforcement learning algorithms for dynamically varying environments. *ACM Comput. Surv.*, 54(6), July 2021. ISSN 0360-0300. doi: 10.1145/3459991. URL <https://doi.org/10.1145/3459991>.
- S. Patel, J. Zhang, N. Narodystka, and S. A. Jyothi. Practically high performant neural adaptive video streaming. *Proc. ACM Netw.*, 2(CoNEXT4), Nov. 2024. doi: 10.1145/3696401. URL <https://doi.org/10.1145/3696401>.
- M. Puderbaugh and P. D. Emmady. Neuroplasticity. In *StatPearls [Internet]*. StatPearls Publishing, 2023.
- G. Sokar, R. Agarwal, P. S. Castro, and U. Evcı. The dormant neuron phenomenon in deep reinforcement learning. In *International Conference on Machine Learning*, pages 32145–32168. PMLR, PMLR, 2023.
- K. Spiteri, R. Urgaonkar, and R. K. Sitaraman. Bola: Near-optimal bitrate adaptation for online videos. *IEEE/ACM transactions on networking*, 28(4):1698–1711, 2020.
- Y. Sun, X. Yin, J. Jiang, V. Sekar, F. Lin, N. Wang, T. Liu, and B. Sinopoli. Cs2p: Improving video bitrate selection and adaptation with data-driven throughput prediction. In *Proceedings of the 2016 ACM SIGCOMM Conference*, pages 272–285, 2016.
- B. Wang, M. Su, W. Wang, K. Chen, B. Liu, F. Ren, M. Xu, J. Liu, and J. Wu. Enhancing low latency adaptive live streaming through precise bandwidth prediction. *IEEE/ACM Transactions on Networking*, 2024a.
- S. Wang, J. Lin, and Y. Dai. Mmvs: Enabling robust adaptive video streaming for wildly fluctuating and heterogeneous networks. *IEEE Transactions on Multimedia*, 2024b.
- S. Wu, C.-X. Wang, M. M. Alwakeel, X. You, et al. A general 3-d non-stationary 5g wireless channel model. *IEEE Transactions on Communications*, 66(7):3065–3078, 2017.
- G. Xu, R. Zheng, Y. Liang, X. Wang, Z. Yuan, T. Ji, Y. Luo, X. Liu, J. Yuan, P. Hua, S. Li, Y. Ze, H. D. III, F. Huang, and H. Xu. Drm: Mastering visual reinforcement learning through dormant ratio minimization. In *The Twelfth International Conference on Learning Representations*. OpenReview.net, 2024. URL <https://openreview.net/forum?id=MSe8YFbhUE>.
- J. Yin, H. Chen, Y. Xu, Z. Ma, and X. Xu. Learning accurate network dynamics for enhanced adaptive video streaming. *IEEE Transactions on Broadcasting*, 70(3):808–821, 2024.
- X. Yin, A. Jindal, V. Sekar, and B. Sinopoli. A control-theoretic approach for dynamic adaptive video streaming over http. In *Proceedings of the 2015 ACM Conference on Special Interest Group on Data Communication*, pages 325–338. ACM, 2015.
- L. Zhao, H. Li, E. Zhang, A. Hawbani, M. Lin, S. Wan, and M. Guizani. Intelligent caching for vehicular dew computing in poor network connectivity environments. *ACM Trans. Embed. Comput. Syst.*, 23(2), Mar. 2024. ISSN 1539-9087. doi: 10.1145/3643038. URL <https://doi.org/10.1145/3643038>.
- T. Zinner, O. Hohlfeld, O. Abboud, and T. Hoßfeld. Impact of frame rate and resolution on objective qoe metrics. In *2010 second international workshop on quality of multimedia experience (QoMEX)*, pages 29–34, Trondheim, 2010. IEEE.

## A Proof of Forward Dormancy Lemma

**Lemma 4.1: (Forward Dormancy Lemma.)** If  $s_{l,i} = 0$ , then  $h_{l,i}(\mathbf{x}) = 0$  for all  $\mathbf{x} \in D$ .

*Proof.* Since  $s_{l,i} = 0$ ,

$$0 = s_{l,i} = \frac{\mathbb{E}_{\mathbf{x} \in D} |h_{l,i}(\mathbf{x})|}{\frac{1}{H_l} \sum_{j=1}^{H_l} \mathbb{E}_{\mathbf{x} \in D} |h_{l,j}(\mathbf{x})|}. \quad (\text{A.1})$$

By the non-degeneracy assumption, the denominator is at least  $m > 0$ . Thus,

$$\mathbb{E}_{\mathbf{x} \in D} |h_{l,i}(\mathbf{x})| = 0. \quad (\text{A.2})$$

Since  $|h_{l,i}(\mathbf{x})| \geq 0$ , the expectation of a nonnegative random variable is zero if and only if the variable is zero almost everywhere. Therefore,

$$h_{l,i}(\mathbf{x}) = 0 \quad \text{for almost all } \mathbf{x} \in D. \quad (\text{A.3})$$

By the continuity of  $h_{l,i}$ , if it were nonzero at any point  $\mathbf{x}_0 \in D$ , continuity would imply a neighborhood around  $\mathbf{x}_0$  where  $h_{l,i}$  remains nonzero, contradicting the almost-everywhere zero condition. Hence,  $h_{l,i}(\mathbf{x}) = 0$  for every  $\mathbf{x} \in D$ .  $\square$

## B Proof of Forward-to-Backward Dormancy Lemma

**Lemma 4.2: (Forward-to-Backward Dormancy Lemma.)** If  $s_{l,i} = 0$ , then  $\Delta h_{l,i}(\mathbf{x}) = 0$  for all  $\mathbf{x} \in D$ .

*Proof.* From Lemma 4.1, we know that if  $s_{l,i} = 0$ ,  $\forall \mathbf{x} \in D$ ,  $h_{l,i}(\mathbf{x}) = 0$ . Let  $\mathbf{x} \in D$  be arbitrary, and consider any perturbation  $\delta_{\mathbf{x}} \in \mathbb{R}^{k_l}$ . By the Mean Value Theorem for vector-valued functions, there exists  $t \in [0, 1]$  such that

$$h_{l,i}(\mathbf{x} + \delta_{\mathbf{x}}) - h_{l,i}(\mathbf{x}) = \nabla h_{l,i}(\mathbf{x} + t\delta_{\mathbf{x}})^T \delta_{\mathbf{x}}. \quad (\text{B.1})$$

Since  $h_{l,i}(\mathbf{x}) = 0$  for every  $\mathbf{x} \in D$ , this difference is zero:

$$0 = \nabla h_{l,i}(\mathbf{x} + t\delta_{\mathbf{x}})^T \delta_{\mathbf{x}}. \quad (\text{B.2})$$

This equality must hold for all  $\mathbf{x} \in D$  and for every possible  $\delta_{\mathbf{x}} \in \mathbb{R}^{k_l}$ . Suppose, for contradiction, that there exists some point  $\mathbf{y} \in D$  where  $\nabla h_{l,i}(\mathbf{y}) \neq 0$ . Take  $\delta_{\mathbf{x}} = \epsilon \nabla h_{l,i}(\mathbf{y})$  for a small  $\epsilon > 0$ , then

$$\nabla h_{l,i}(\mathbf{y} + t\epsilon \nabla h_{l,i}(\mathbf{y}))^T (\epsilon \nabla h_{l,i}(\mathbf{y})) = 0. \quad (\text{B.3})$$

As  $\epsilon \rightarrow 0$ , continuity of  $\nabla h_{l,i}$  ensures  $\nabla h_{l,i}(\mathbf{y} + t\epsilon \nabla h_{l,i}(\mathbf{y})) \rightarrow \nabla h_{l,i}(\mathbf{y})$ , which is nonzero by assumption. Hence the inner product  $\nabla h_{l,i}(\mathbf{y})^T (\epsilon \nabla h_{l,i}(\mathbf{y}))$  would not vanish for small  $\epsilon \neq 0$ , yielding a contradiction. Thus, no such  $\mathbf{y}$  can exist, and we conclude

$$\nabla h_{l,i}(\mathbf{x}) = 0 \quad \forall \mathbf{x} \in D. \quad (\text{B.4})$$

$\square$

## C Proof of Backward Dormancy Lemma

**Lemma 4.3: (Backward Dormancy Lemma)** Suppose the gradient  $\nabla h_{l,i}(\mathbf{x}) = 0$  for all  $\mathbf{x} \in \mathcal{X}_l$ . Then  $h_{l,i}(\mathbf{x})$  is constant on  $\mathcal{X}_l$ . Moreover, if  $h_{l,i}(\mathbf{x}) = 0$  at any point  $\mathbf{x}_0 \in \mathcal{X}_l$ , then  $h_{l,i}(\mathbf{x}) = 0$  for all  $\mathbf{x} \in \mathcal{X}_l$ , and hence the neuron is dormant ( $s_{l,i} = 0$ ).

*Proof.* Since  $\nabla h_{l,i}(\mathbf{x}) = 0$  for every  $\mathbf{x} \in \mathcal{X}_l$ . Then  $h_{l,i}$  does not change with respect to  $\mathbf{x}$ . By standard multivariable calculus, any function whose gradient is zero everywhere on a connected domain must be constant. Concretely, for any two points  $\mathbf{x}_1, \mathbf{x}_2 \in \mathcal{X}_l$ , we have

$$h_{l,i}(\mathbf{x}_2) - h_{l,i}(\mathbf{x}_1) = \int_{\mathbf{x}_1}^{\mathbf{x}_2} \nabla h_{l,i}(\mathbf{u}) d\mathbf{u} = 0, \quad (\text{C.1})$$

indicating  $h_{l,i}(\mathbf{x}_2) = h_{l,i}(\mathbf{x}_1)$ . Therefore,  $h_{l,i}(\mathbf{x})$  is constant on  $\mathcal{X}_l$ . Denote this constant by  $c$ , so  $h_{l,i}(\mathbf{x}) = c$  for all  $\mathbf{x} \in \mathcal{X}_l$ .

Next, assume there exists a point  $\mathbf{x}_0 \in \mathcal{X}$  such that  $h_{l,i}(\mathbf{x}_0) = 0$ , then  $c = 0$ . Hence  $h_{l,i}(\mathbf{x}) = 0$  for every  $\mathbf{x} \in \mathcal{X}_l$ . In particular, for  $\mathbf{x} \in D \subseteq \mathcal{X}_l$ , we have  $h_{l,i}(\mathbf{x}) = 0$ . Consequently,

$$\mathbb{E}_{\mathbf{x} \in D} |h_{l,i}(\mathbf{x})| = 0 \quad \implies \quad s_{l,i} = \frac{0}{\frac{1}{H_H} \sum_k \mathbb{E}_{\mathbf{x} \in D} |h_{l,k}(\mathbf{x})|} = 0. \quad (\text{C.2})$$

Thus the neuron is fully dormant.

**Remark.** If  $c \neq 0$ , then  $\mathbb{E}_{\mathbf{x} \in D} |h_{l,i}(\mathbf{x})|$  would be  $|c| \neq 0$ , so  $s_{l,i}$  could potentially be nonzero, indicating the neuron is not dormant. Therefore, the key condition that  $h_{l,i}(\mathbf{x}) = 0$  at some point  $\mathbf{x}_0 \in \mathcal{X}_l$  (thus forcing  $c = 0$ ) is crucial to concluding  $s_{l,i} = 0$ . In many network architectures, one can ensure  $h_{l,i}(0) = 0$  by design (e.g., bias initialized to zero and activation is ReLU), or rely on data/architectural constraints that force a zero constant rather than a nonzero one.  $\square$

## D Proof of Bidirectional Dormancy Characterization

**Theorem 4.4: (Bidirectional Dormancy Characterization)** Let  $D \subseteq \mathcal{X}_l \subseteq \mathbb{R}^{k_l}$  be the domain from which inputs  $\mathbf{x}$  are drawn. Consider layer  $l$  with  $H_l$  neurons. For the  $i$ -th neuron in layer  $l$ , let

$$h_{l,i}(\mathbf{x}) = \sigma_l(\mathbf{w}_{l,i}^T \mathbf{x} + b_{l,i}), \quad (\text{D.1})$$

where  $\sigma_l$  is continuously differentiable and applied elementwise. The neuron's *dormancy index* is defined as:

$$s_{l,i} = \frac{\mathbb{E}_{\mathbf{x} \in D} |h_{l,i}(\mathbf{x})|}{\frac{1}{H_l} \sum_{j=1}^{H_l} \mathbb{E}_{\mathbf{x} \in D} |h_{l,j}(\mathbf{x})|}. \quad (\text{D.2})$$

**Assume:**

1. (Continuity and Differentiability)  $h_{l,i}(\mathbf{x})$  is in  $C^1(\mathbb{R}^{k_l})$ .
2. (Boundedness)  $\exists M > 0: \mathbb{E}_{\mathbf{x} \in D} |h_{l,i}(\mathbf{x})| \leq M$ .
3. (Non-degeneracy)  $\exists m > 0: \frac{1}{H_l} \sum_{j=1}^{H_l} \mathbb{E}_{\mathbf{x} \in D} |h_{l,j}(\mathbf{x})| \geq m$ .

Then the following two statements are equivalent:

- (A) **Dormancy:**  $s_{l,i} = 0$ . Equivalently,  $\mathbb{E}_{\mathbf{x} \in D} |h_{l,i}(\mathbf{x})| = 0$ .
- (B) **Zero Gradient (on  $D$ ) plus at least one zero activation:**

$$\nabla h_{l,i}(\mathbf{x}) = 0 \quad \forall \mathbf{x} \in D \quad \text{and} \quad \exists \mathbf{x}_0 \in D: h_{l,i}(\mathbf{x}_0) = 0. \quad (\text{D.3})$$

*Proof. (A)  $\Rightarrow$  (B):* Suppose  $s_{l,i} = 0$ . By Lemma 4.1,  $h_{l,i}(\mathbf{x}) = 0$  for all  $\mathbf{x} \in D$ . Then by the Lemma 4.2, we get  $\nabla h_{l,i}(\mathbf{x}) = 0$  for all  $\mathbf{x} \in D$ . Clearly, in this scenario, pick  $\mathbf{x}_0 \in D$  arbitrarily;  $h_{l,i}(\mathbf{x}_0) = 0$ . Thus the right-hand side of the equivalence is satisfied. *(A)  $\Leftarrow$  (B):* Conversely, assume  $\nabla h_{l,i}(\mathbf{x}) = 0$  for all  $\mathbf{x} \in D$  and there exists at least one point  $\mathbf{x}_0 \in D$  where  $h_{l,i}(\mathbf{x}_0) = 0$ . Since  $\nabla h_{l,i} \equiv 0$  on  $D$ , the neuron's output  $h_{l,i}$  is constant throughout  $D$ . That constant must be zero (as it is zero at  $\mathbf{x}_0$ ). Hence  $h_{l,i}(\mathbf{x}) = 0$  for all  $\mathbf{x} \in D$ . By Lemma 4.1 (applied in reverse logic), if the neuron is identically zero on  $D$ , then  $s_{l,i} = 0$ .  $\square$

## E Silent Neuron Characterization

**Theorem 4.5: (Silent Neuron Characterization)** Let  $D \subseteq \mathcal{X}_l \subseteq \mathbb{R}^{k_l}$  be the domain from which inputs  $\mathbf{x}$  are drawn. Consider layer  $l$  with  $H_l$  neurons. For the  $i$ -th neuron in layer  $l$ , let

$$h_{l,i}(\mathbf{x}) = \sigma_l(\mathbf{w}_{l,i}^T \mathbf{x} + b_{l,i}), \quad (\text{E.1})$$

where  $\sigma_l$  is continuously differentiable and applied elementwise. The neuron's *activity index* is defined as:

$$\xi_{l,i} = \frac{\mathbb{E}_{\mathbf{x} \in D} |h_{l,i}(\mathbf{x})| \cdot \mathbb{E}_{\mathbf{x} \in D} |g_{l,i}(\mathbf{x})|}{\frac{1}{H_l} \sum_{j \in h} (\mathbb{E}_{\mathbf{x} \in D} |h_{l,j}(\mathbf{x})|)}, \quad (\text{E.2})$$

where  $g_{l,i}(\mathbf{x}) = \frac{\partial}{\partial h_{l,i}} \sum_i f_\theta(\mathbf{x}_i)$  represents the neuron's gradient computed from the aggregated network outputs. Assume:

1. (Continuity and Differentiability)  $h_{l,i}(\mathbf{x})$  and  $g_{l,i}(\mathbf{x})$  are in  $C^1(\mathbb{R}^{k_l})$ .
2. (Boundedness)  $\exists M_h, M_g > 0: \mathbb{E}_{\mathbf{x} \in D} |h_{l,i}(\mathbf{x})| \leq M_h$  and  $\mathbb{E}_{\mathbf{x} \in D} |g_{l,i}(\mathbf{x})| \leq M_g$ .
3. (Non-degeneracy)  $\exists m > 0: \frac{1}{H_l} \sum_{j=1}^{H_l} \mathbb{E}_{\mathbf{x} \in D} |h_{l,j}(\mathbf{x})| \geq m$ .

Then for an arbitrarily small constant  $\epsilon > 0$ , the following statements are equivalent:

- (A) **Silence:**  $\xi_{l,i} < \epsilon$ .
- (B) **Zero Forward and Backward Activity (on  $D$ ):**

$$\mathbb{E}_{\mathbf{x} \in D} |h_{l,i}(\mathbf{x})| < \sqrt{\epsilon} \quad \text{and} \quad \mathbb{E}_{\mathbf{x} \in D} |g_{l,i}(\mathbf{x})| < \sqrt{\epsilon}. \quad (\text{E.3})$$

*Proof.* (A)  $\Rightarrow$  (B): Assume  $\xi_{l,i} < \epsilon$ . Then:

$$\begin{aligned}
& \epsilon > \xi_{l,i} \\
& = \frac{\mathbb{E}_{\mathbf{x} \in D} |h_{l,i}(\mathbf{x})| \cdot \mathbb{E}_{\mathbf{x} \in D} |g_{l,i}(\mathbf{x})|}{\frac{1}{H_l} \sum_{j \in h} (\mathbb{E}_{\mathbf{x} \in D} |h_{l,j}(\mathbf{x})|)} \\
& \geq \frac{\mathbb{E}_{\mathbf{x} \in D} |h_{l,i}(\mathbf{x})| \cdot \mathbb{E}_{\mathbf{x} \in D} |g_{l,i}(\mathbf{x})|}{M_h} \quad (\text{By Boundedness}) \\
& = \frac{1}{M_h} \cdot \mathbb{E}_{\mathbf{x} \in D} |h_{l,i}(\mathbf{x})| \cdot \mathbb{E}_{\mathbf{x} \in D} |g_{l,i}(\mathbf{x})|.
\end{aligned}$$

Therefore,  $\mathbb{E}_{\mathbf{x} \in D} |h_{l,i}(\mathbf{x})| \cdot \mathbb{E}_{\mathbf{x} \in D} |g_{l,i}(\mathbf{x})| < M_h \epsilon$ . Since both terms are non-negative, we must have  $\mathbb{E}_{\mathbf{x} \in D} |h_{l,i}(\mathbf{x})| < \sqrt{M_h \epsilon}$  and  $\mathbb{E}_{\mathbf{x} \in D} |g_{l,i}(\mathbf{x})| < \sqrt{M_h \epsilon}$ . As  $\epsilon$  can be arbitrarily small, this implies (B).

(B)  $\Rightarrow$  (A): Assume (B) holds. Then:

$$\begin{aligned}
\xi_{l,i} & = \frac{\mathbb{E}_{\mathbf{x} \in D} |h_{l,i}(\mathbf{x})| \cdot \mathbb{E}_{\mathbf{x} \in D} |g_{l,i}(\mathbf{x})|}{\frac{1}{H_l} \sum_{j \in h} (\mathbb{E}_{\mathbf{x} \in D} |h_{l,j}(\mathbf{x})|)} \\
& < \frac{\sqrt{\epsilon} \cdot \sqrt{\epsilon}}{m} \quad (\text{By Non-degeneracy and (B)}) \\
& = \frac{\epsilon}{m}.
\end{aligned}$$

As  $\epsilon$  can be arbitrarily small, this implies  $\xi_{l,i} < \epsilon$  for any  $\epsilon > 0$ , proving (A).  $\square$

## F ReSiN Algorithm

In this section, we will introduce Algorithm 1 (ReSiN), which is designed to periodically detect and reinitialize silent neurons during the training of a policy network. This is done in order to maintain the expressivity of the neural network. In our implementation, we have decoupled the computation of gradient-based metrics  $\xi_{l,i}^g$  and dormancy output  $\xi_{l,i}^d$  indicators in order to facilitate a more detailed performance analysis.

---

### Algorithm 1 ReSiN: Reset Silent Neurons Algorithm

---

**Require:** Policy and Value network parameters  $\theta$ , neuron activation threshold  $\epsilon$ , maximum training iterations  $T$ , update frequency  $F$

```

1: for iteration  $t = 1$  to  $T$  do
2:   Execute interaction to obtain trajectories
3:   if  $t \bmod F == 0$  then
4:     Perform policy gradient optimization on  $\theta$ 
5:     for each neural unit  $i$  in hidden layers do
6:       if activation intensity  $\xi_{l,i}^g \leq \epsilon_1$  and  $\xi_{l,i}^d \leq \epsilon_2$  then
7:         Initialization to afferent connections of unit  $i$ 
8:         Zero-init all efferent connections from unit  $i$ 
9:       end if
10:    end for
11:   end if
12: end for

```

---

## G Ablation Experiment

To validate the effectiveness and generality of our proposed ReSiN framework, we conducted comprehensive ablation studies focusing on the Reset mechanism. In particular, we evaluated ReSiN’s performance by varying the gradient reset thresholds and dormancy thresholds.

To assess the overall performance of the algorithm, we conducted ablation studies using various learning rates. The result is shown in Fig. 9, 10, 11.

Our proposed approach has consistently demonstrated superior QoE across a range of learning rates and reset thresholds.

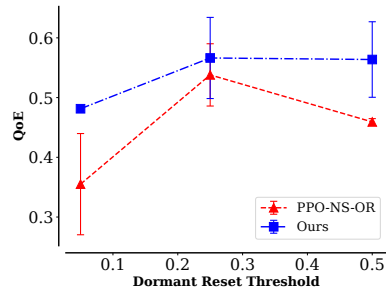


Figure 9: Performance comparison under different dormant Reset threshold.

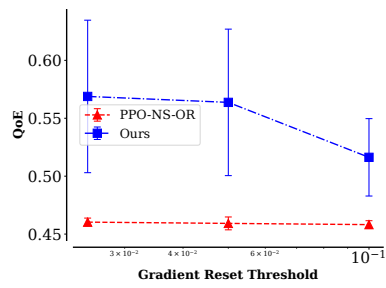


Figure 10: Performance comparison under different gradient Reset threshold.

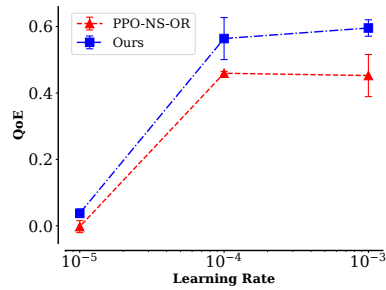


Figure 11: Performance comparison under different learning rates.